Dynamic Scheduling of Approximate Telemetry Queries

Chris Misa
University of Oregon

Walt O'Connor
University of Oregon

Ramakrishnan Durairajan
University of Oregon

Reza Rejaie
University of Oregon

Walter Willinger
NIKSUN, Inc.

Abstract

Network telemetry systems provide critical visibility into the state of networks. While significant progress has been made by leveraging programmable switch hardware to scale these systems to high and time-varying traffic workloads, less attention has been paid towards efficiently utilizing limited hardware resources in the face of dynamics such as the composition of traffic as well as the number and types of queries running at a given point in time. Both these dynamics have implications on resource requirements and query accuracy.

In this paper, we argue that this dynamics problem motivates reframing telemetry systems as *resource schedulers*—a significant departure from state-of-the-art. More concretely, rather than statically partition queries across hardware and software platforms, telemetry systems ought to decide on their own and at runtime *when* and for *how long* to execute the set of active queries on the data plane. To this end, we propose an efficient approximation and scheduling algorithm that exposes accuracy and latency tradeoffs with respect to query execution to reduce hardware resource usage. We evaluate our algorithm by building *DynATOS*, a hardware prototype built around a reconfigurable approach to ASIC programming. We show that our approach is more robust than state-of-the-art methods to traffic dynamics and can execute dynamic workloads comprised of multiple concurrent and sequential queries of varied complexities on a single switch while meeting per-query accuracy and latency goals.

1 Introduction

Network telemetry systems provide users (e.g., network operators, researchers) with critical insights into the state of the network by collecting information about individual packets and processing this information into high-level features in near real-time. Typically, these features are the results of user-defined queries, where a query is expressed as a sequence of high-level operations such as filter and reduce [22, 33, 43]. Generated query results drive management decisions such as deploying defensive measures in the face of an attack or updating routing to avoid congestion. A key functionality of telemetry systems is to determine how best to leverage available resources (*e.g.*, network hardware resources, such as switch ASICs or NICs; software-programmable resources, such as general-purpose CPUs) to execute a given set of queries. Due to massive traffic volumes and often stringent timing requirements, state-of-the-art telemetry systems typically make use of programmable network hardware (*e.g.*, programmable switch ASICs [2, 4, 5]) and also apply approximation techniques (*e.g.*, sketches [24, 38, 39]).

In executing user-defined queries, telemetry systems must cope with two independent and challenging sources of dynamics. First, the resources required to execute any given query depend on the underlying distributions (*i.e.*, composition) of network traffic. For example, a DDoS-detection query that counts the number of sources contacting each destination might require a counter for each destination active on the network, but the number of active destinations may vary over time [38]. The accuracy guarantees of state-of-the-art approximation techniques like sketches [39] likewise depend on traffic distributions so that if these distributions change, accuracy can no longer be guaranteed. Second, the number and type of concurrent queries submitted by a user can vary over the system's deployment. For example, an operator might need to submit followup queries to pinpoint the root cause of increased congestion. Both these sources of dynamics affect data plane resource usage implying that telemetry systems must dynamically adjust resource allocations.

Several recent efforts [38, 43] have made progress towards coping with both of these sources of dynamics individually and in isolation, but do not address challenges arising from their simultaneous presence in network telemetry systems. For example, ElasticSketch [38] presents a method for dynamically coping with changes in traffic rate and distribution. However, this effort relies on a fixed flow key which forces users to reload the switch pipeline to change queries. On the other hand, Newton [43] describes a technique to update query operations during runtime which enables users to dynamically add and remove queries as their monitoring needs change. However, Newton does not consider the problem of adjusting resource allocations between concurrent queries as traffic composition changes. To the best of our knowledge, no recent work addresses these simultaneous sources of dynamics in an efficient switch hardware based system.

In this work, we argue that, in order to simultaneously address these sources of dynamics, *telemetry systems should be reframed as active resource schedulers for query operations*. In particular, telemetry systems must manage finite switch hardware processing resources while adapting to varying numbers and types of queries as well as varying traffic composition. To support this argument, we make the following key contributions.

Time-division approximation method. Viewing telemetry systems as online schedulers enables a new approximation technique based on time-division approximation. At a high-level, this technique observes that query operations do not need to run all the time. Instead, operations can execute during strategically placed sub-windows of the overall time window (*e.g.*, an operation could execute for 3 of 8 equal-duration sub-windows of a 5 s overall time window). This technique is grounded in cluster sampling theory which allows us to estimate error and future resource requirements.

Adaptive scheduling algorithm. We provide a closed loop adaptive scheduling algorithm which leverages time-division approximation to execute operations from many user-defined queries on a single switch ASIC. Our scheduling algorithm leverages multi-objective optimization to balance between multiple high-level goals such as prioritizing accuracy, latency, or reduced volume of reported data across queries.

Evaluation in a functional hardware prototype. To evaluate our proposed techniques, we implement *DynATOS*,[1] a telemetry operation scheduling system which leverages programmable switch hardware to answer dynamically submitted queries. Our current implementation of *DynATOS* assumes a single runtime programmable switch hardware capable of executing a restricted number of primitive operations as supported by a telemetry module found in a widely available off-the-shelf switch ASIC. We evaluate *DynATOS* on our hardware prototype and through simulation showing that (i) time-division approximation is more robust than sketches to changes in traffic dynamics while offering a similar accuracy, overhead tradeoff space, (ii) our adaptive scheduler is able to meet query accuracy and latency goals in the presence of traffic and query dynamics, and (iii) the overheads in our scheduling loop are minimal and dominated by the time required to report and process intermediate results from the switch—an overhead which can be mitigated significantly by leveraging fully programmable switch hardware.

[1]*DynATOS* stands for Dynamic Approximate Telemetry Operation Scheduler.

2 Background & Motivation

2.1 Dynamic Telemetry Use Cases

Example 2.1. Consider a scenario where a telemetry system is executing the DDoS and port scanning detection tasks described in Sonata [22][2]. The first stage of these tasks finds a set of distinct elements in each time window or epoch (*e.g.*, IPv4 source, destination pairs every epoch for DDoS). Suppose traffic follows a stable pattern for several epochs with only small changes in the number of distinct elements considered by both tasks and that the telemetry system adjusts resource allocations for these two queries to achieve good accuracy. Now, suppose at some later epoch traffic changes so that a much larger number of sources are seen (either due to a natural event like a flash crowd or due to an actual DDoS attack). This larger number of sources increases the number of pairs that both queries must keep track of and either more resources will need to be allocated or accuracy will suffer.

While this example only considered a pair of queries, in realistic settings operators likely need to monitor for a wide variety of attacks simultaneously (*e.g.*, the 11 queries described in Sonata [22]). Moreover, features like number of sources or destinations commonly overlap in these types of attack detection queries so that an anomalous change in one feature may upset the resource requirements of a large number of simultaneous queries.

Example 2.2. Consider a scenario where a network operator wants to understand the root cause of TCP latency on their network. In this scenario, the operator would like to first run queries to detect when latency increases and for which hosts or subnets [18]. Once detected, the operator must submit a large number of queries to test possible causes of high latency such as re-transmissions or deep queues [33] with filter operations so that these queries only apply to the flows experiencing latency. Note that the debugging phase may require several rounds of querying with tens of simultaneous queries in each round before the root cause of the latency can be determined.

While the above examples focus on two particular tasks, the underlying concepts—of dealing with large shifts in query resource requirements caused by changes in traffic and of executing multiple queries over time in a dependent manner—are commonly encountered in network operations.

2.2 Ideal Telemetry System Requirements

In light of the above-mentioned examples, an ideal telemetry system should support the following requirements.

R1: Query diversity. Marple [33] and Sonata [22] outline how a small set of parameterized stream processing operators can enable a wide range of telemetry queries. Telemetry systems must support these kinds of generic query description interfaces, allowing filtering over packet header values,

[2]The DDoS task finds destinations receiving from large numbers of distinct sources and the port scanning task finds sources sending to a large number of distinct destination ports.

Approach	R1	R2	R3	R4	R5
Static switch-based	✓				✓
Runtime-programmable	✓	✓		✓	✓
Dynamic allocation		✓	✓	✓	✓
Sketch-based	✓	✓			✓
Software-based	✓	✓	✓	✓	
DynATOS	✓	✓	✓	✓	✓

Table 1: Summary of how different approaches relate to the requirements of § 2.2.

grouping by arbitrary header fields, chaining operations, and joining the results of multiple operation chains.

R2: Approximate execution. Executing telemetry queries over the massive volumes of data flowing through networks poses heavy resource requirements. Furthermore, many telemetry queries are equally effective when computed approximately [30]. Therefore, telemetry systems should expose approximation techniques that allow trading off reduced result accuracy for lower resource requirements.

R3: Traffic dynamics. Composition of traffic changes over time, and changes may be slow, regular, and easy to predict (*e.g.*, daily cycles) or fast and hard to predict (*e.g.*, flash crowds). As discussed in Example 2.1, these changes in traffic composition lead to changes in the resource requirements for different groups of queries. Telemetry systems should robustly handle these changes without compromising query accuracy or latency [38].

R4: Query dynamics. The queries a network operator needs to run change over time. Some of these changes may be infrequent (*e.g.*, adding new queries to monitor a newly deployed service), while some of these changes may be rapid and time-sensitive (*e.g.*, adding new queries to debug a performance anomaly or to pinpoint and block a network attack). Telemetry systems should be able to handle these dynamic query arrivals and removals, realizing updates within a few milliseconds and without incurring network downtime [43].

R5: Switch hardware acceleration. Due to massive traffic volumes, stringent timing requirements, and the limited speed of a single CPU core, executing telemetry queries on CPU-based systems is prohibitively expensive [22]. As a result, telemetry systems must leverage resource-constrained hardware targets [2, 4, 5] to accelerate query execution.

2.3 State-of-the-art and their Limitations

State-of-the-art approaches each satisfy a subset of the requirements set forth above, but face limitations which hinder their ability to satisfy all requirements simultaneously.

Static switch-based approaches. Marple [33] and Sonata [22] compile traffic queries into static hardware description languages like P4 [10], demonstrating the efficiency of switch hardware in computing query results. However, these approaches fail to satisfy R4 since changing queries incurs seconds of network downtime (see [43]).

Runtime-programmable approaches. Recently, Beau-Coup [14] and Newton [43] demonstrate techniques to allow network operators to add and remove queries at runtime without incurring downtime. These efforts lay a technical foundation to address R4, but do not address the challenge of R3.

Dynamic allocation approaches. DREAM [30] and SCREAM [31] develop dynamic allocation systems for telemetry operations addressing both R3 and R4. However, these approaches do not satisfy R1 because they require query-specific accuracy estimators.

Sketch-based approaches. Many telemetry efforts address R2 by leveraging sketches [15, 16, 28, 39, 42] to gather approximate query results under the stringent operation and memory limitations faced in the data plane. However, the accuracy of sketches is tightly coupled to both the resources allocated (*e.g.*, number of hash functions or number of counters) and the underlying composition of traffic (*e.g.*, number of flows) making sketches insufficient for R3 and R4. An exception to this is ElasticSketch [38] which addresses R3 head on by dynamically adapting to varying traffic compositions. However, ElasticSketch fails to address R4 or R1 since flow keys are fixed in the sketch's implementation.

Software-based approaches. Several prior efforts leverage the capabilities of general-purpose CPUs to process traffic queries. For example, Trumpet [32] installs triggers on end hosts, OmniMon [25] and switch pointer [37] share tables between end hosts and switches in network, and SketchVisor [23] and NitroSketch [27] tune sketch-based approximation techniques for virtual switches. While these approaches work well in settings like data centers where all infrastructure is under a single administrative domain, in many settings (*e.g.*, campus or enterprise networks) it is too expensive (in terms of infrastructure cost and/or latency) to pass all packets through software and impractical to instrument end hosts.

Scheduling distributed stream processing operations. Several efforts [26, 34–36, 41] address the challenge of efficiently scheduling stream processing operations to maximize resource utilization. However, these efforts do not consider the particular types of accuracy and latency constraints encountered in scheduling telemetry operations on switch hardware.

Limitations of current hardware-based approaches. To illustrate the limitations of current static approaches [22, 33, 43] in dealing with R3 and R4, we implement the two queries mentioned in Example 2.1 and run them over a traffic excerpt from the MAWILab [17] data set which features pronounced traffic dynamics. This excerpt starts with relatively stable traffic, then suddenly, due to an actual DDoS attack or other causes (which we do not claim to identify), around the 20^{th} 5 s time window (or *epoch*) contains a large number of sources sending regular pulses of traffic. As suggested in [22, 43], we use bloom filters tuned for the initial normal traffic to approximate the lists of distinct pairs required by the first stage of both queries.

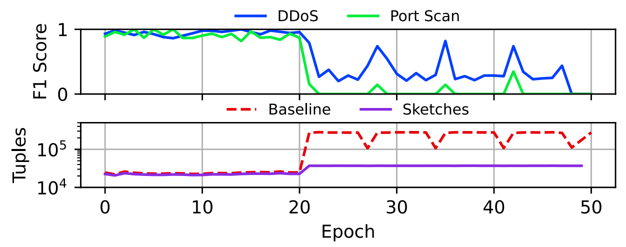

Figure 1: Accuracy of concurrent DDoS and port scanning queries under extreme traffic dynamics.

Figure 1 shows the F1 score[3] of these approximate query implementations along with the number of tuples returned to the collector in each epoch. Before the change in number of sources, the approximation methods for both queries return highly accurate results while sending relatively few tuples. However, when the number of sources increases, the approximation accuracy of both queries suffers since the actual number of ground truth tuples (the "Baseline" trace) far exceeds the number each query was tuned for. Taking the static approach in this example shows that *when certain events of interest occur, the accuracy of multiple queries can be significantly impacted due to fixed assumptions about traffic composition.* Of course, the telemetry system initially could have tuned these queries for the anticipated number of sources, but this would lead to significant wastage of resources under normal traffic conditions and it is hard to know what to tune for without prior knowledge of the anomaly.

2.4 Design Challenges

To elucidate why prior efforts fail to meet the requirements put forth in § 2.2, we next describe the following high-level design challenges.

D1: Approximating generic query results. Efforts like Marple and Sonata develop expressive query description languages which map into data plane computation models. However, approximation of query operations is often necessary due to limited data plane resources and massive traffic volumes. It is unclear how state-of-the-art approximation methods can be leveraged to work with queries expressed in languages like Marple or Sonata. As illustrated in § 2.3, the currently proposed baseline approach of simply replacing stateful reductions in Sonata queries with sketch-based primitives requires prior knowledge of worse-case traffic situations and does not perform well under dynamic traffic scenarios.

D2: Estimating accuracy of approximations. Approximate query results must be accompanied with a sound estimate of their accuracy. This is critical for operators to understand the system's confidence in detecting a particular event or reporting a particular metric and equally critical in dynamic telemetry systems to inform the balance of resources between approximate queries. Prior efforts have made progress towards this goal [24, 30, 31], but none anticipate accuracy estimation for current state-of-the-art generic query descriptions.

D3: Allocating finite hardware resources among variable sets of queries under traffic dynamics. Very few prior efforts address the need of a telemetry system to evaluate multiple concurrent queries on finite hardware resources. In order to handle traffic dynamics, such a system must dynamically update resource allocations based on the estimated accuracy of each query. Moreover, since it is possible that the given resources will be insufficient to meet the accuracy of all queries, such a system must enable operators to express query priorities and allocate resources with respect to these priorities.

3 *DynATOS* System Design

3.1 Overview

To tackle the above-mentioned challenges, we build *DynATOS*. At its core, *DynATOS* is composed of three main components as shown in Figure 2. Network operators submit queries to the scheduler through a high-level REST API which performs initial query validation and returns a status message along with a description of the expected query result format. The scheduler then translates queries into their primitive operations and constructs schedules for how these operations should be run on switch hardware. These schedules are then handed to a runtime component which communicates with switch hardware to execute the primitive operations and collect intermediate results. Once ready, the runtime component gathers all results and passes them back to the scheduler and operators.

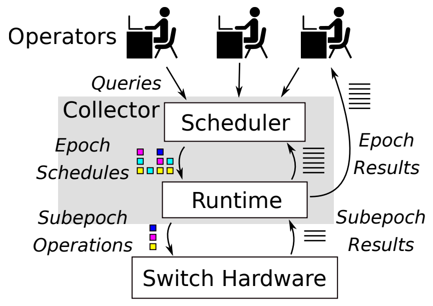

Figure 2: Architecture of *DynATOS*.

3.2 Preliminaries

Scheduling horizon. Since queries can arrive at any time, we must decide when and for how far into the future resources should be scheduled. We first examine several possible approaches to this problem, then describe our approach in the next paragraph. One option is to compute the schedule each time a new query arrives and adjust all existing queries to the new schedule. While this option minimizes the time a query has to wait before it can start executing, it complicates the realization of accuracy and latency goals since the duration of the scheduling horizon (*i.e.*, until the next query arrives) is unknown when forming the schedule. Alternatively, we could compute the new schedule each time all queries in the prior

[3] Computed by comparing with ground truth, the F1 score is a measure of query accuracy defined as the harmonic mean of precision and recall.

schedule terminate. While this option ensures schedules can be executed exactly as planned, newly submitted queries may experience a longer delay.

We choose, instead, to make scheduling decisions at fixed windows of time which we call *epochs* (*e.g.*, every 5 s). This allows a balance between the two schemes mentioned above: queries must wait at most the duration of one epoch before executing and during an epoch queries are ensured to execute according to the schedule. In particular, we divide the scheduling epoch into N subepochs and our scheduler assigns subsets of the submitted queries to each subepoch as shown in Figure 3. Subepochs provide flexibility to schedule different queries at different times while also providing concrete resource allocation units. Queries submitted during an epoch are checked for feasibility and only considered in the following epoch. For example, in the figure, Q4 is added sometime during epoch 2, but cannot be scheduled until epoch 3. During the epoch, the scheduler collects intermediate results for each subepoch in which a query is executed and aggregates these subepoch results based on the query's aggregation operation. Once an epoch completes, results of complete queries are returned, while new and incomplete queries are considered for the next epoch. For example, in Figure 3 Q3 completes execution in the second subepoch of epoch 2 and its results are returned during the scheduler invocation before epoch 3. We further assume that each query executes over traffic in a single epoch and telemetry tasks requiring longer measurement durations than our scheduling epoch can simply re-submit queries.

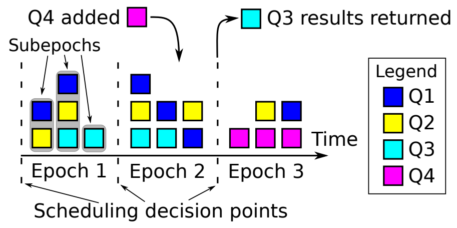

Figure 3: Example of scheduling 4 queries with $N = 3$ subepochs per epoch.

3.3 Key Ideas

We develop a novel approximation method to address the challenge of gathering approximate results for generic queries (D1). In particular, our method leverages cluster sampling theory to estimate the results of the first aggregation operator in multistage queries. For example, in the DDoS query we only approximate computation of the distinct source, destination pairs list and execute all subsequent operations exactly. The intuition behind this is that each operator in a telemetry query tends to reduce the volume of data passed to the next operator. Therefore, reducing the resource requirements and volume of data emitted from the first aggregation reduces the load on all subsequent operators.

§ 4 describes how our approximation method can provide sound estimates of result accuracy without prior assumptions about traffic characteristics (addressing D2). Note that the accuracy estimates used in many sketch methods are dependent on traffic characteristics (which can be estimated by auxiliary queries or offline analysis) [39]. Our method, on the other hand, uses cluster sampling to estimate result accuracy based on observations from a single epoch independently of traffic characteristics. Moreover, by leveraging observations of feature variance in prior epochs, we can predict resource requirements for a desired accuracy level in future epochs. This feedback loop allows our system to dynamically adjust per-query allocations as traffic distributions change.

To address D3, we integrate our approximation technique in a scheduler that determines how a number of concurrent queries should be executed on a single switch hardware, balancing resources between queries to satisfy accuracy and latency goals set by operators. As described in § 5, our scheduler uses a novel multi-objective optimization formulation of the problem of when to run which queries given query priorities and resource constraints. This formulation allows the scheduler to balance between the goals of multiple concurrent queries, sometimes allocating less than the exact number of subepochs when queries have lower priority and resources are scarce (*e.g.*, due to a large number of concurrent queries).

Finally, we develop a runtime system leveraging these ideas to efficiently execute schedules on switch hardware, gather intermediate results, apply factors to correct for sampling, and return results to network operators in a high-level format. Operators can then decide to execute new queries in the subsequent epoch, or to re-execute the current queries based on these results.

3.4 Limitations and Assumptions

Monitoring problems addressed by *DynATOS*. The types of traffic features which can be monitored by queries in *DynATOS* are subject to the following assumptions.

- Feature values do not fluctuate excessively over measurement durations of one or two seconds.
- The monitoring task can be implemented using features gathered at a single point in the network.
- Features are constructed from packet header fields and/or other switch-parsable regions of the packet.
- Features can be computed using atomic filter, map, and reduce operations.

Under these assumptions monitoring tasks like detecting microbursts [13], identifying global icebergs [19], and detecting patterns in TCP payloads [9] cannot be efficiently executed using *DynATOS*. However, as evidenced by the body of prior efforts with similar assumptions (*e.g.*, [22, 30, 33]) and the concrete examples discussed in § 2.1, *DynATOS* can still be used for a wide variety of useful tasks.

Switch hardware model. In the following, we assume a restricted runtime programmable switch hardware model. In this model, switch hardware is able to execute a fixed set of Sonata [22] operators, in particular, a filter operator followed by a reduce operator. However, similar to Newton [43], our switch hardware allows arbitrary parameterization of these operators *at runtime*. For example, switch hardware could execute the filter and reduce commands required by the Sonata TCP new connections queries for a period of time, then quickly (*e.g.*, within a few milliseconds) be re-programmed to execute the filter and reduce commands required by the Sonata DDoS query. We note that our scheduling methods are independent of this particular switch hardware model and could readily be applied to more fully programmable ASICs [5,10].

Network-wide scheduling. Ultimately, operators need to query traffic across different logical or physical domains of their network. This implies that telemetry systems should collect information from a distributed set of switches (or other monitoring points) and provide a global view of network traffic. In this work, we consider only a single monitoring point (*e.g.*, a critical border switch) and leave the challenges of distributed scheduling of telemetry operations to future work. Nonetheless, a single switch deployment on a enterprise or data center border switch can still be highly effective in executing the types of queries considered.

4 Time-Division Approximation in *DynATOS*

Accuracy tradeoff. Given fixed scheduling epochs, we can trade off accuracy for reduced resource requirements by sampling a subset of the subepochs in which to execute a particular query. We leverage cluster sampling theory [29] to expose this tradeoff while maintaining accuracy goals. Cluster sampling is a good fit for situations like dynamically scheduled query operations where the cost of sampling large groups of the population (*i.e.*, subepochs) is significantly lower than the cost of sampling individual population members (*i.e.*, packets) [29]. In particular, we assume sending the aggregate results (computed in switch hardware) of each sampled subepoch to software is cheaper than sending individual sampled packets to software.

Consider the case where a particular query executes in n of the N total subepochs and let $t_{i,j}$ be the query's result in the i-th subepoch of the j-th epoch, n_j be the number of subepochs in which the query executed in the j-th epoch, E be the total number of epochs in which the query is executed, and $s^2_{t_j}$ be the sample variance of the $t_{i,j}$'s in the j-th epoch. We use the unbiased estimator,[4]

$$\hat{t}_E = \frac{1}{E}\sum_{j=1}^{E}\hat{t}_j = \frac{1}{E}\sum_{j=1}^{E}\frac{N}{n_j}\sum_{i\in S_j} t_{i,j} \tag{1}$$

which has standard error

$$SE(\hat{t}_E) = \frac{N}{E}\sqrt{\sum_{j=1}^{E}\left(1-\frac{n_j}{N}\right)\frac{s^2_{t_j}}{n_j}} \tag{2}$$

[4]See § A for a full discussion of the derivation of these equations from cluster sampling theory.

to estimate query results and determine when accuracy goals have been fulfilled. We rearrange Equation 2 as

$$n^{acc} = \frac{s^2_{t_E} N^2}{E^2\sigma^2 - \left(\sum_{j=1}^{E-1}\operatorname{Var}(\hat{t}_j)\right) + N s^2_{t_E}} \tag{3}$$

to estimate the number of subepochs in which a query should execute in the E-th epoch to fulfill a given standard error target σ assuming the query has already executed in the previous $E-1$ epochs without fulfilling σ. Note that if $\sigma = 0$, then $n^{acc} = N$ and the query will be executed in all of the subepochs in its first epoch. As σ increases, n^{acc} decreases freeing more of the subepochs for other queries.

Latency tradeoff. In addition to the accuracy tradeoff discussed above, we can tradeoff result latency for reduced resource requirements by executing a query's operations across several epochs. The key observation enabling this tradeoff is that by spreading the sampled subepochs over several epochs, the query can reduce its per-epoch requirements while still attaining its accuracy goal. Operators leverage this tradeoff by specifying larger latency goals on queries that do not require fast returns.

Suppose a particular query has a latency goal of $\tilde{E}$ epochs. We need to estimate the number of subepochs in which the query should be allocated n^{lat} in the e-th epoch with $1 \le e \le \tilde{E}$. First, we break the sum in Equation 2 into *past* ($1 \le j < e$) and *future* ($e < j \le \tilde{E}$) components. We then have,

$$n^{lat} = \frac{s^2_{t_E} N^2}{\tilde{E}^2\sigma^2 - N^2\left(past + future\right) + N s^2_{t_E}} \tag{4}$$

While the *past* component can be calculated directly using observations from prior epochs, the *future* component must be estimated based on the number of subepochs the query expects to receive in future epochs. Operators can tune this expected number of subepochs based on current and expected query workloads.

Correcting distinct operators. While the previous sections discuss foundations for making sound approximations of packet/byte counts, many useful queries also involve identifying and counting distinct elements. We leverage the Chao estimator without replacement[5] to correct estimates of a common class of distinct count queries such as the DDoS query considered in § 2.1. Similar to the cluster sampling estimators described in this section, the Chao estimator can be used to obtain point and standard error estimates based only on the observed sample.

5 Scheduling in *DynATOS*

5.1 Optimization Formulation

We cast the task of generating query schedules as an optimization problem and adapt well-known techniques to generate

[5]See § A.3 for details.

schedules through this casting. While this section details our casting of the problem, § 5.2 describes the challenges inherent in applying optimization techniques in a real-time setting such as ours.

We apply our optimization formulation every epoch to determine which queries should execute in each of the N subepochs as shown in Algorithm 1. First, in line 2 we use the DISENTANGLE method of Yuan et al. [40] to break the submitted queries Q into disjoint traffic slices K and save the mapping between queries and slices in $s_{i,k}$. Line 3 then computes the minimum number of stateful update operations required by the reduce operators of all queries in each particular slice. These steps are necessary given our single-stage switch hardware model (§ 3.4). Next, lines 4 through 6 compute estimates of the memory and subepoch requirements of each query. Finally line 7 creates and solves the optimization problem described below. If a feasible solution cannot be found, line 9 falls back to a heuristic scheduling method described in § 5.2.

Algorithm 1 Method for determining subepoch schedule

```
1:  procedure GET-SCHEDULE($Q$, $u$, $SE$)
2:      $K, s \leftarrow$ DISENTANGLE($Q$)
3:      $U \leftarrow$ COMBINE-UPDATES($u, K, s$)
4:      $m \leftarrow$ ESTIMATE-MEMORY
5:      $n^{acc} \leftarrow$ EQUATION 3($\sigma$)
6:      $n^{lat} \leftarrow$ EQUATION 4($\sigma, E$)
7:      $d \leftarrow$ SOLVE-OPTIMIZATION
8:      if $d$ is infeasible then
9:          $d \leftarrow$ GET-HEURISTIC-SCHEDULE
10:     end if
11: end procedure
```

Inputs. Table 2 shows the particular inputs and outputs of this optimization problem. Of the input variables, t_k, u_i, $s_{i,k}$, T, A, and M are known exactly based on submitted query requirements and available switch resources, while m_i, n_i^{acc}, and n_i^{lat} must be estimated based on observation of past epochs. Our current implementation uses EWMA to estimate m_i and $s_{t_E}^2$ (as required by n_i^{acc} and n_i^{lat}) independently for all update operation types. We leave exploration of more sophisticated estimation approaches to future work. Scheduling decisions are encoded in the $d_{i,j}$ indicator variables which determine which queries should execute in each subepoch. We do not consider the division of switch memory between queries since memory is dynamically allocated during the aggregation operation (see § 3.4).

Constraints. We impose the constraints shown in Table 3 to satisfy two high-level requirements: (i) respecting switch resource limits (C1, C2, C3) and (ii) forcing minimal progress in each query and ensuring variance estimates are well-defined (C4). Note that C2 captures the fact that if two queries rely on the same update operation, they can be merged to use a single ALU. In the case that the estimated quantity m_i turns out to be violated by traffic conditions in the subsequent epoch, we simply drop new aggregation groups once the available switch memory is totally consumed.

Objectives. In computing the schedule of each epoch, we consider the objective functions listed in Table 4. O1 seeks to satisfy accuracy goals by minimizing the distance to the value of n^{acc} computed in Equation 3, O2 seeks to satisfy latency goals by minimizing the distance to the value of n^{lat} computed in Equation 4, and O3 seeks to limit the maximum volume of data that needs to be returned from the switch in a single subepoch. We expose the Pareto front of these objective functions using linear scalarization which allows operators to express the importance of each objective by submitting weights and is computationally efficient.

Variable	Description
Q	index set of queries ready for execution
SE	index set of subepochs
K	index set of all disjoint traffic slices
U_k	index set of all update operations in slice k
t_k	number of TCAM entries required by slice k
u_i	index of update operation required by query i
$s_{i,k}$	indicator that query i requires slice k
m_i	memory required in each subepoch by query i
n_i^{acc}	number of subepochs required for accuracy goal for query i (§ 4)
n_i^{lat}	number of subepochs required for latency goal for query i (§ A.2)
T	total available TCAM entries
A	total number of available switch ALUs
M	total available SRAM counters
$d_{i,j}$	indicator that query i executes in subepoch j

Table 2: Variables used in optimization formulation of scheduling problem. The sole outputs $d_{i,j}$ determine the schedule for the next epoch.

$$\textbf{C1:} \quad \forall j \in SE, \ \sum_{k \in K} t_k \mathbf{I}\left[\bigvee_{i \in Q} d_{i,j} s_{i,k} = 1\right] \leq T$$

$$\textbf{C2:} \quad \forall j \in SE, \ k \in K, \ \sum_{u \in U_k} \mathbf{I}\left[\bigvee_{i \in Q} d_{i,j} s_{i,k} \mathbf{I}[u_i = u] = 1\right] \leq A$$

$$\textbf{C3:} \quad \forall j \in SE, \ \sum_{i \in Q} d_{i,j} m_i \leq M$$

$$\textbf{C4:} \quad \forall i \in Q, \ \sum_{j \in SE} d_{i,j} \geq 2$$

Table 3: Scheduling problem constraints to respect (C1) TCAM capacity requirement, (C2) switch ALU capacity, (C3) SRAM capacity, and (C4) query minimal progress requirement. $\mathbf{I}[]$ is the indicator function.

$$\textbf{O1:} \quad \text{minimize} \sum_{i \in Q} \left| \left(\sum_{j \in SE} d_{i,j} \right) - n_i^{acc} \right|$$

$$\textbf{O2:} \quad \text{minimize} \sum_{i \in Q} \left| \left(\sum_{j \in SE} d_{i,j} \right) - n_i^{lat} \right|$$

$$\textbf{O3:} \quad \text{minimize} \sum_{i \in Q, j \in SE} d_{i,j} m_i$$

Table 4: Objective functions considered in the multi-objective formulation.

5.2 Challenges of Online Optimization

Unlike prior work (*e.g.*, [22]), the inputs to our optimization problem are dependent on task dynamics (*e.g.*, the set Q can vary each epoch) and traffic dynamics (*e.g.*, the suggested n_i^{acc} could increase in response to increased traffic variability). Hence, we must solve the optimization problem independently in each epoch. However, invoking an optimization solver in an online scheduling method is fraught with challenges. First, certain combinations of inputs and constraints can lead to infeasible problems where it is impossible to satisfy all constraints. Second, since integer programming is a well known NP-complete problem, finding an optimal solution can take exponential time in the worst case. In what follows, we describe several precautions that we take in the design of our scheduler to ensure these challenges do not adversely affect the performance of the telemetry system.

Dealing with infeasible queries. Our first strategy to deal with infeasible optimization problems is to require that all submitted queries can be executed on the given switch resources in the absence of other queries. In particular, if a query requires more than T TCAM entries, A ALUs, or M counters, the scheduler must reject that query outright, since it will not be able to execute on the given switch hardware. This ensures that our scheduler can always make progress on the current pool of submitted queries by selecting a single query and allocating the full switch resources for all subepochs. We note that a query partition scheme similar to Sonata [22] could be added to our system to handle this case more elegantly, but leave this to future work.

Dealing with slow optimizations. To deal with the potentially exponential time that could be required to converge to an optimal solution, we limit the duration of time spent in the optimization algorithm to an acceptable fraction of total epoch time. This method, known as early stopping, is a well-known technique to gather feasible, good, if not fully optimal solutions. When the optimization process stops due to this time limit, the current solution must still be checked for feasibility and only allowed to execute if it is, in fact, feasible.

Fail-safe. In cases where the optimization problem is either proven infeasible or times out before converging, we fall back to a simple heuristic "fail-safe" mode of scheduling. We also deny all new query submissions when in fail-safe mode to notify the operator that the system is currently saturated and to prevent the accumulation of a large backlog which could cause the optimization problem to remain infeasible in future epochs. Our simple heuristic fail-safe scheduling scheme greedily selects the query closest to its deadline and allocates this query fully to switch resources. To increase progress in fail-safe mode, we also add other queries that use the same or a subset of the selected query's traffic slices until either the memory or ALU limit is reached. Since queries scheduled in this mode execute for each subepoch, $n_j/N = 0$ for that epoch ensuring progress towards accuracy targets, though some queries may suffer increased latency.

Another approach to dealing with situations where a feasible schedule cannot be found is to send slices of traffic to the collector and compute query results in software. In this approach queries running during fail-safe mode could still meet tight latency goals at the expense of increased load on the collector. Depending on the nature of situation triggering fail-safe mode, this could impose infeasible processing loads on the collector or lead to excessive congestion between switch and collector. In future work, we plan to investigate solutions to this problem including combinations of heuristic scheduling and moving query operations to software.

6 Evaluation

In this section, we describe our evaluation of *DynATOS* and demonstrate the following key results.

- The time-division approximation technique in *DynATOS* is more robust than state-of-the-art in the face of traffic dynamics and offers comparable performance to state-of-the-art sketch-based approximate techniques (§ 6.2).
- The scheduling method in *DynATOS* handles dynamic query workloads with up to one query every second and leverages specific accuracy and latency goals to reduce per-query resource usage (§ 6.3).
- Latency overheads in *DynATOS* are minimal and dependent on the load on the collector and the number of queries which must be updated in switch hardware (§ 6.4).

6.1 Experimental Setup

Setting. We evaluate *DynATOS* on a BCM 56470 series [8] System Verification Kit (SVK) switch running BroadScan [1] which implements the telemetry operations described in § 3.4. Our version of BroadScan has $A = 8$ parallel ALU operators, and a flow table with $M \approx 9$MB of memory. A software agent on the switch's CPU manages reconfiguration of hardware in response to requests from the collector. Our collector and scheduling software runs on a server with an Intel Xeon Gold 5218 CPU at 2.3Ghz and 383GB memory. This server is equipped with a 40Gb Mellanox MT27700-family network card connected directly to the SVK's data plane. A separate 10Gb Intel X550T network card on the same server connects to the SVK's management interface to manage updates to hardware configuration as schedules execute.

Traces. Unless otherwise stated, we replay a trace from the MAWILab traffic data set (Sept. 1st, 2019) [17] using `tcpreplay` [7]. We selected this trace as a baseline because some of its features are static while others are more dynamic.

Default parameters. We use five-second scheduling epochs to allow sufficient measurement duration without incurring excessive delay of results which must wait for epoch boundaries. We divide epochs into $N = 8$ subepochs so that the schedule has sufficient options for arranging queries without making subepochs too short to generate useful samples. We set objective weights to balance between priorities and suppose queries will get all future subepochs when evaluating

Equation 4. Queries are submitted with realistic values of σ based on baseline measurements of their variances in the trace. We set $\alpha = 1/2$ in the EWMA estimation described in § 5.1. Bars show median and error bars show 5th and 95th percentiles over all epochs of the trace.

Query workloads. We use *DynATOS* to implement four of the telemetry queries originally introduced by Sonata [22] and used in several recent efforts. Our hardware model handles a fixed sequence of filter and reduction operations so we implement the remaining query operations in software. This scenario is equivalent to Sonata with a limited number of switch hardware stages. We report the accuracy of approximate implementations of these queries as F1 score (the harmonic mean of precision and recall) by comparing against ground truth computed offline. In addition to static queries, we generate dynamic query workloads based on random processes to evaluate *DynATOS* (see § 6.3). To the best of our knowledge, there is no comparable publicly-available dynamic query workload benchmark. Our workloads are publicly released at [6] to support validation of our results and to facilitate benchmarking of similar systems in the future.

Implementation. We implement the *DynATOS* scheduler in ~14k lines of C and C++. Following ProgME [40], we use BDDs to represent query filter conditions in our implementation of the DISENTANGLE algorithm (§ 5.1). We use the open source CBC implementation [3] to solve the optimization problems described in § 5.1. Our implementation also defers some result processing operations to the time spent waiting for results from switch hardware to improve efficiency.

Comparisons. We compare *DynATOS* with ElasticSketch [38], Newton [43], and SketchLearn [24]. We modified the implementations of both ElasticSketch and SketchLearn to support the filter and reduce operations required by several of the Sonata [22] queries. Though we were unable to locate a publicly available implementation of Newton, we implemented its sketch-based approach to approximating Sonata's primitive operators. In particular, we use count-min sketch [15] to approximate the `reduce` operator and a bloom filter [20] to approximate the `distinct` operator.

6.2 Performance of Time-Division Approximation

Robustness in the face of traffic dynamics. To address the question of what happens when traffic composition changes significantly we consider an excerpt from the MAWILab dataset taken on Nov. 14th, 2015. As shown in Figure 4, this excerpt features nominally static traffic followed by a dramatic surge in the number of sources around 100 seconds into the trace.

To understand how different methods handle this change in traffic dynamics, we first tune each method's parameters to achieve high accuracy (F1 > 0.9) on the first 100 seconds of the excerpt, then run the method with these parameters over the entire excerpt. Since it is possible that this anomaly

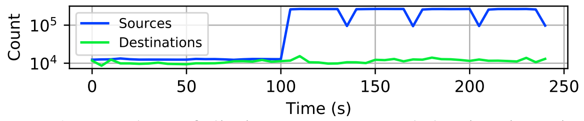

Figure 4: Number of distinct sources and destinations in excerpt from MAWILab data on Nov. 14th, 2015.

was cause by some form of DDoS attack, we run the DDoS query in this scenario to locate the victim of the attack. This is intended to reflect a realistic situation where a method was deployed and tuned for a particular traffic composition, which then changes. In real deployments, such changes could be caused by attacks or performance anomalies and represent the moments when data collected from a telemetry system is most critical.

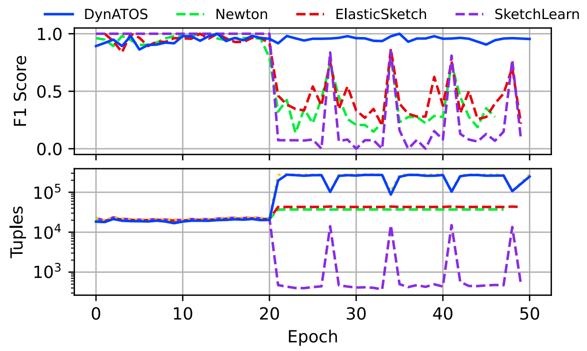

Figure 5: Performance of different methods on the 2015 MAWILab excerpt shown in Figure 4.

Figure 5 shows the F1 score and number of tuples returned to the collector in each epoch over the trace excerpt. All methods achieve high accuracy for the first 20 epochs, but then when the number of sources increases after the 20th epoch, they diverge significantly. First, we note that *DynATOS* is able to maintain high accuracy where other methods suffer by dynamically increasing the load on the collector. This is a result of the natural robustness of our non-parametric sampling method: when the underlying traffic composition changes, those changes are reflected in each sampled subepoch causing the volume of data reported for each subepoch to increase to ensure steady accuracy.

The sketch-based methods in ElasticSketch and Newton, on the other hand, are limited by the static table sizes configured for the first 20 epochs: once the traffic composition changes, these tables become saturated and excessive hash collisions lead to F1 scores below 0.5. We confirm that the average number of hash collisions per epoch jumps by 2× when the traffic distribution changes in epoch 21. We note that these sketch-based methods also offer no easy way to estimate the accuracy of returned results, so while an operator may become suspicious due to the slight increase in load on the collector, they would have no way to verify that the accuracy of these methods is compromised.

Sketchlearn differs from other methods in that it reconstructs flow keys based on data stored in a multi-level sketch.

Sketchlearn guarantees only that it will be able to extract all flows that make up more than $1/c$ of the total traffic where c is the fixed number of columns in the sketch. We confirm that in this trace, the increased number of sources is caused by a large number of small flows (one to two packets). As such, the threshold to be extracted increases, but none of the added flows are able to meet it and so SketchLearn is unable to extract existing as well as new flows with high enough confidence. SketchLearn does associate accuracy estimates with these results so an operator could be notified of this situation, but would have to reload their switch's pipeline with a larger value of c in order to achieve acceptable accuracy.

Overall accuracy-load tradeoff. As in previous efforts [22], we consider the volume of data returned from switch hardware to the collector (*i.e.*, load on the collector) as a critical resource. Each approximation method can reduce this load while reducing accuracy of query results, leading to a performance curve in accuracy vs. load space. To empirically estimate this curve, we determine several different parameterizations of each method, execute the method with each parameterization over all epochs of the trace, then compute the accuracy and load on collector in each epoch. For some queries the sketch-based methods must export their full sketches to the collector so we report load in terms of both tuples (the number of records or events) and bytes (the total size of data). We use the median of each value over all epochs to estimate the empirical performance curves.

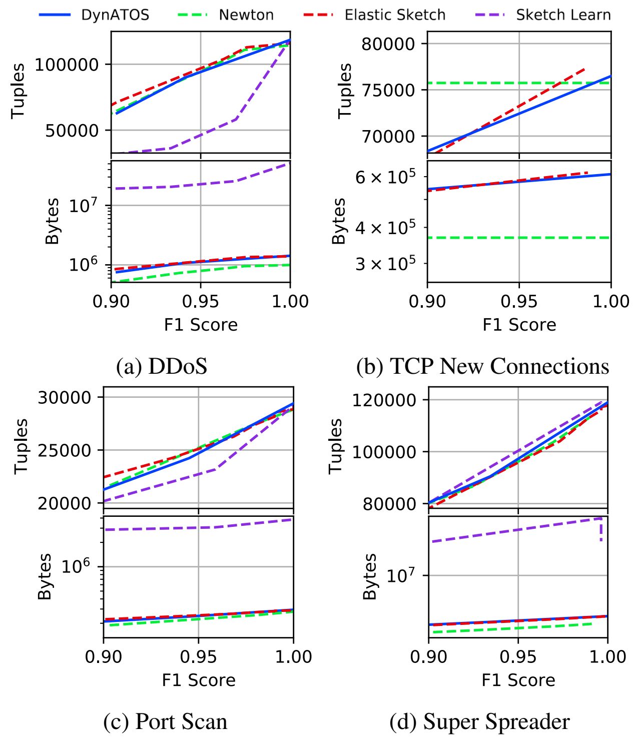

Figure 6: Accuracy vs. overhead curves.

Figure 6 shows performance curves for four different queries with two plots for each query showing overhead as tuples and bytes on the *y*-axis. Here we use the baseline MAWILab trace so these results represent a mostly static traffic scenario. Note that the lower right-hand corner of these plots is ideal with maximal accuracy and minimal load. We observe that *DynATOS*' novel approximation method (§ 4) performs as well as, if not better than other methods. The sketch-based method proposed by Newton achieves slightly better performance in terms of total data volume on the DDoS and Super Spreader queries because it only sends flow keys from the first distinct operator whereas other methods also return a counter. SketchLearn requires relatively large multi-level sketches to be exported each epoch in order to achieve comparable accuracy on these queries despite it's lower tuple counts. In the case of TCP new connections, we were unable to run a large enough sketch to reach the accuracy range shown here for other methods. We observe that for the TCP new connections query Newton's count-min sketch is highly sensitive to sketch size. For example, adding a single additional counter moves the F1 score across the entire range shown in the plot. *DynATOS*, on the other hand, achieves comparable if not higher performance and offers a wider range of load savings.

6.3 Performance of Scheduling Algorithm

Dynamic query workload. Real telemetry system deployments must deal with dynamics in the number and types of queries submitted to the network over time. Since, to the best of our knowledge, no representative dynamic query workloads are available, we synthesize such workloads based on the following scheme. First, we generate a series of base queries with random aggregation keys and granularities and arrival times based on a Poisson process with rate λ. We suppose these base queries are submitted by a human operator or automated process which then submits followup queries based on base query results. In particular, when each base query terminates, we submit between 0 and 3 followup queries with the same aggregation as the base query, but filters added to select a single aggregation group from the base query's results. For example, if a base query with aggregation key source IP address at 8 bit granularity returned results for 0.0.0.0/8, 10.0.0.0/8, and 192.0.0.0/8, we might submit followup queries to monitor just 10.0.0.0/8 and 192.0.0.0/8. To provide contrasting accuracy and latency goals, base queries are submitted with looser accuracy goals ($\sigma = 100$) and latency goals randomly chosen within a range of 1 to 5 epochs, while followup queries are submitted with tighter accuracy goals ($\sigma = 50$) and a latency goal of 1 epoch.

Figure 7 shows the evolution of the number of queries submitted by one of our dynamic query workloads (top plot) and traces of different operating metrics (lower three plots). In this workload, the maximum number of queries is submitted in epoch 8 which leads to an infeasible schedule since too many TCAM entries are required to keep track of all filter groups of followup queries. This causes our scheduler to enter fail-safe mode for two epochs to dispatch with the excess queries. Note

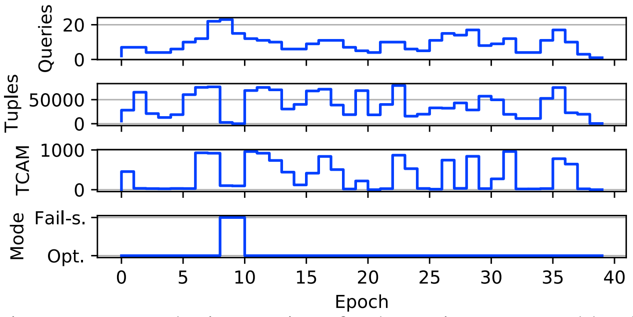

Figure 7: Example time-series of a dynamic query workload (3/5 queries per second).

that the heuristic algorithm currently used to select queries in fail-safe mode only selects a few queries based on fully disjoint traffic slices leading to reduction of load on collector and TCAM utilization. Under the software-based fail-safe mode mentioned in § 5.2, the load on collector would continue increasing here while TCAM utilization would drop.

To understand how *DynATOS* scales with the rate of dynamic query workloads, we generate a set of five workloads with different base query arrival rates. Figure 8 shows how these different workload intensities affect the performance of *DynATOS* in terms of queries served (Queries), tuples emitted to the collector (Tuples), TCAM entries used (TCAM), epochs spent in fail-safe mode (% Fail-s.), and the percentage of satisfied queries (% Sat.) all per-epoch. We count the number of queries satisfied as the total number of queries that received valid results during the workload run. Note that some queries submitted when the scheduler is in fail-safe mode are denied at submission time allowing an operator to re-submit these queries later. In these experiments we observe that all successfully submitted queries receive results within their target accuracy and latency goals.

We observe that, as expected, the number of queries serviced, load on collector, and number of TCAM entries required all scale linearly with the base query rate. As also expected, the number of queries satisfied decreases as more epochs are spent in fail-safe mode. We observe that the main contributor to infeasible scheduling problems in this scenario is the number of TCAM entries required to satisfy followup queries' filter conditions. We plan to investigate integration of more efficient TCAM allocation algorithms in future work to address this bottleneck.

Relaxation of accuracy & latency goals. Next, we evaluate how our approximation and scheduling method is able to reduce the per-query resource requirements in response to relaxed accuracy and latency goals. We execute the TCP new connections query with varying accuracy and latency goals and measure resource usage over 10 epochs at each setting. Here we report ALU-seconds and counter-seconds which combine both the number of ALUs (or counters) used by the query and the duration for which these resources were used.

Figure 9 show the resulting resource usages as both accuracy and latency goals vary in the form of heatmaps. These

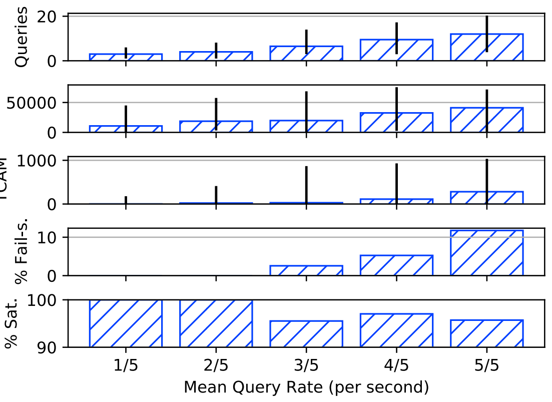

Figure 8: Performance of *DynATOS* on dynamic query workloads.

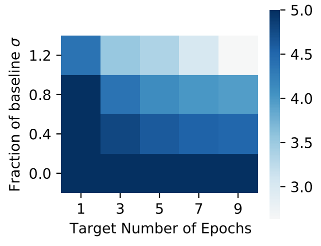

(a) ALU-seconds

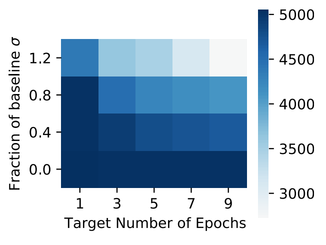

(b) counter-seconds

Figure 9: Evaluation of median resource usages for selected accuracy (y-axis) and latency (x-axis) targets for a single query. Lighter colors indicate lower resource usages.

results demonstrate that both accuracy and latency goals can help *DynATOS* leverage our time-division approximation method to reduce resource requirements.

6.4 Scheduling loop overheads

Closed-loop systems like *DynATOS* must quickly gather results and update switch hardware configurations between each subepoch in order to avoid missing potentially critical traffic. We define the inter-epoch latency as the total time spent not waiting for results from switch hardware. In other words, the inter-epoch latency is the total time taken by our system to gather results, reconfigure hardware operations, and decide which operations to execute in the next epoch. We observe two distinct factors that contribute to the inter-epoch latency: the load on the collector and the number of queries installed in switch hardware.

Latency vs. load on collector. The first factor contributing to inter-epoch latency is the volume of data that must be returned and processed after each subepoch. To isolate this effect, we generate synthetic traffic consisting of a certain number of sources each sending a steady stream of packets controlled by a Poisson process. We then run a query that returns a single record for each source so that by varying the number of sources in the traffic, we directly control the number of records returned and hence the load on collector.

Figure 10 shows the distribution of total latency for two different loads. We observe that the median inter-epoch la-

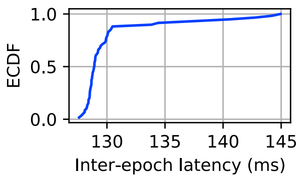

(a) 10 Records

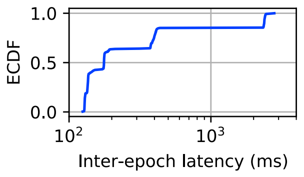

(b) 10^5 Records

Figure 10: Distribution of inter-epoch latency in our testbed system for different loads on the collector.

tency in both cases is less than 130 ms, but that with higher load the tail latencies grow to over a second. This is likely due to that fact that the collector code must allocate larger memory blocks to process the increased number of tuples returned from the switch. We leave a full investigation of the performance of our software collector to future work.

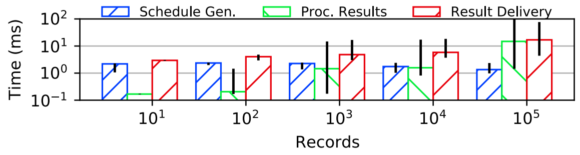

Figure 11: Software overheads as function of tuples exported.

We further investigate how the different components of our query scheduler impact this overall inter-epoch latency by instrumenting the scheduler. Figure 11 shows the latency break down as a function of the number of records processed for three key components: the time to generate a schedule for the epoch (Schedule Gen.), the time spent processing intermediate results at the end of the epoch (Proc. Results), and the time spent sending results back to the query-submitting process (Result Delivery). The results demonstrate that the main variable software latency is the time to process results which scales nearly linearly with the number of records. A more significant bottleneck is imposed by the result delivery time due to the use of a simple REST protocol which requires new TCP connections and data marshaling via JSON. We leave exploration of more efficient IPC mechanisms for this interface to future work.

Latency vs. number of queries. The second main factor contributing to inter-epoch latency is the time required to install and remove query operations on switch hardware. This factor is influenced primarily by the amount of state which must be written into hardware memory which is a function of the number of queries to be installed or removed. We generate synthetic workloads containing different numbers of disjoint queries based again on the TCP new connections query and instrument our switch agent to measure the time taken by writes into hardware memory.

Figure 12 shows the time taken by the hardware writes to add and remove operations (Add Hw. and Remove Hw.) as well as the total time taken by the switch agent (Add Tot. and Remove Tot.) which includes the time to deserialize and validate configurations sent from the collector. These results show that up to 100 queries can be added or removed on our prototype in ∼10 ms (comparable to latencies reported in prior efforts [30, 43]). We also observe that the deserialization and validation conducted by the switch agent imposes minimal overhead. Finally, the total contribution of switch hardware to the overall inter-epoch latency is dominated by operation removal. This is because when removing operations, the switch agent must also reset the entire flow table used by these operations so as to avoid future operations anomalously reporting leftover results.

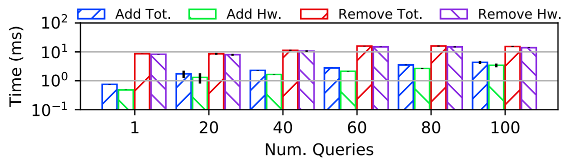

Figure 12: Hardware overheads as function of number of queries.

7 Conclusion and Future Work

Current approaches to telemetry system design struggle to efficiently satisfy dynamism in query workloads and traffic workload composition. By reframing telemetry systems as resource schedulers, in this work, we propose an efficient approximation and scheduling algorithm that exposes accuracy and latency tradeoffs with respect to query execution to reduce hardware resource usage. We evaluate our algorithm by building *DynATOS* and show that our approach is more robust than state-of-the-art methods to traffic dynamics and dynamic query workloads.

While we investigate the common sources of dynamics, both a *horizontal scheduling problem* (*i.e.*, how to design a scheduler to deal with those dynamics for multiple switch hardware stages or multiple distributed switches) and a *vertical scheduling problem* (*i.e.*, incorporation of computing resources, such as stream processing clusters and GPUs—both locally and at remote cloud data centers—into the pool of resources schedulable for telemetry tasks) remain. This opens up a wider question of *where*, not just *when* and *for how long*, telemetry queries should be executed. We plan to investigate this question as part of future work.

Acknowledgments

We thank our shepherd (Behnaz Arzani) and the anonymous reviewers for their constructive feedback. We also thank Shahram Davari and Broadcom, Inc. for providing hardware and technical support for our testbed evaluation. This work is supported by the National Science Foundation through CNS 1850297, a Ripple faculty fellowship, and a Ripple graduate fellowship. The views and conclusions contained herein are those of the authors and should not be interpreted as necessarily representing the official policies or endorsements, either expressed or implied, of NSF, Ripple, or Broadcom.

References

[1] BCM56275 Gb/s Programmable Multilayer Switch Product Brief. https://docs.broadcom.com/doc/56275-PB.

[2] BCM56870 series. https://www.broadcom.com/products/ethernet-connectivity/switching/strataxgs/bcm56870-series.

[3] COIN-OR Branch-and-cut MIP solver. https://zenodo.org/badge/latestdoi/30382416.

[4] Intel ethernet switch FM6000 series product brief. https://www.intel.com/content/dam/www/public/us/en/documents/product-briefs/ethernet-switch-fm6000-series-brief.pdf.

[5] Intel Tofino. https://www.intel.com/content/www/us/en/products/network-io/programmable-ethernet-switch.html.

[6] ONRG: DynATOS. https://onrg.gitlab.io/projects/dynatos/.

[7] Tcpreplay - Pcap editing and replaying utilities. https://tcpreplay.appneta.com/.

[8] Trident3-X4 / BCM56470 Series. https://www.broadcom.com/products/ethernet-connectivity/switching/strataxgs/bcm56470-series.

[9] Kevin Borders, Jonathan Springer, and Matthew Burnside. Chimera: A declarative language for streaming network traffic analysis. In *Proceedings of the USENIX Security Symposium*, pages 365–379, 2012.

[10] Pat Bosshart, Dan Daly, Glen Gibb, Martin Izzard, Nick McKeown, Jennifer Rexford, Cole Schlesinger, Dan Talayco, Amin Vahdat, George Varghese, et al. P4: Programming protocol-independent packet processors. *ACM SIGCOMM Computer Communication Review*, 44(3):87–95, 2014.

[11] Anne Chao and Chun-Huo Chiu. Species richness: estimation and comparison. *Wiley StatsRef: Statistics Reference Online*, pages 1–26, 2014.

[12] Anne Chao and Chih-Wei Lin. Nonparametric lower bounds for species richness and shared species richness under sampling without replacement. *Biometrics*, 68(3):912–921, 2012.

[13] Xiaoqi Chen, Shir Landau Feibish, Yaron Koral, Jennifer Rexford, and Ori Rottenstreich. Catching the microburst culprits with snappy. In *Proceedings of the ACM Workshop on Self-Driving Networks*, pages 22–28, 2018.

[14] Xiaoqi Chen, Shir Landau-Feibish, Mark Braverman, and Jennifer Rexford. Beaucoup: Answering many network traffic queries, one memory update at a time. In *Proceedings of the conference of the ACM Special Interest Group on Data Communication (SIGCOMM)*, pages 226–239, 2020.

[15] Graham Cormode and Shan Muthukrishnan. An improved data stream summary: the count-min sketch and its applications. *Journal of Algorithms*, 55(1):58–75, 2005.

[16] Cristian Estan, George Varghese, and Mike Fisk. Bitmap algorithms for counting active flows on high speed links. In *Proceedings of the ACM SIGCOMM conference on Internet measurement (IMC)*, pages 153–166, 2003.

[17] Romain Fontugne, Pierre Borgnat, Patrice Abry, and Kensuke Fukuda. MAWILab: Combining Diverse Anomaly Detectors for Automated Anomaly Labeling and Performance Benchmarking. In *Proceedings of the ACM Conference on emerging Networking EXperiments and Technologies (CoNEXT)*, 2010.

[18] Sriharsha Gangam, Jaideep Chandrashekar, Ítalo Cunha, and Jim Kurose. Estimating TCP latency approximately with passive measurements. In *Proceedings of the International Conference on Passive and Active Measurement (PAM)*, pages 83–93. Springer, 2013.

[19] Sriharsha Gangam, Puneet Sharma, and Sonia Fahmy. Pegasus: Precision hunting for icebergs and anomalies in network flows. In *Proceedings of the IEEE International Conference on Computer Communications (INFOCOM)*, pages 1420–1428, 2013.

[20] Shahabeddin Geravand and Mahmood Ahmadi. Bloom filter applications in network security: A state-of-the-art survey. *Computer Networks*, 57(18):4047–4064, 2013.

[21] Nicholas J Gotelli and Robert K Colwell. Estimating species richness. *Biological diversity: frontiers in measurement and assessment*, 12:39–54, 2011.

[22] Arpit Gupta, Rob Harrison, Marco Canini, Nick Feamster, Jennifer Rexford, and Walter Willinger. Sonata: Query-driven streaming network telemetry. In *Proceedings of the conference of the ACM Special Interest Group on Data Communication (SIGCOMM)*, pages 357–371, 2018.

[23] Qun Huang, Xin Jin, Patrick PC Lee, Runhui Li, Lu Tang, Yi-Chao Chen, and Gong Zhang. Sketchvisor: Robust network measurement for software packet processing. In *Proceedings of the conference of the ACM Special Interest Group on Data Communication (SIGCOMM)*, pages 113–126, 2017.

[24] Qun Huang, Patrick PC Lee, and Yungang Bao. Sketchlearn: Relieving user burdens in approximate measurement with automated statistical inference. In *Proceedings of the conference of the ACM Special Interest Group on Data Communication (SIGCOMM)*, pages 576–590, 2018.

[25] Qun Huang, Haifeng Sun, Patrick PC Lee, Wei Bai, Feng Zhu, and Yungang Bao. Omnimon: Re-architecting network telemetry with resource efficiency and full accuracy. In *Proceedings of the conference of the ACM Special Interest Group on Data Communication (SIGCOMM)*, pages 404–421, 2020.

[26] Teng Li, Jian Tang, and Jielong Xu. Performance modeling and predictive scheduling for distributed stream data processing. *IEEE Transactions on Big Data*, 2(4):353–364, 2016.

[27] Zaoxing Liu, Ran Ben-Basat, Gil Einziger, Yaron Kassner, Vladimir Braverman, Roy Friedman, and Vyas Sekar. Nitrosketch: Robust and general sketch-based monitoring in software switches. In *Proceedings of the conference of the ACM Special Interest Group on Data Communication (SIGCOMM)*, pages 334–350. 2019.

[28] Zaoxing Liu, Antonis Manousis, Gregory Vorsanger, Vyas Sekar, and Vladimir Braverman. One sketch to rule them all: Rethinking network flow monitoring with univmon. In *Proceedings of the 2016 ACM SIGCOMM Conference*, pages 101–114. ACM, 2016.

[29] Sharon L Lohr. *Sampling: Design and Analysis: Design And Analysis*. CRC Press, 2019.

[30] Masoud Moshref, Minlan Yu, Ramesh Govindan, and Amin Vahdat. DREAM: Dynamic resource allocation for software-defined measurement. *ACM SIGCOMM Computer Communication Review*, 44(4):419–430, 2014.

[31] Masoud Moshref, Minlan Yu, Ramesh Govindan, and Amin Vahdat. SCREAM: Sketch resource allocation for software-defined measurement. In *Proceedings of the ACM Conference on emerging Networking EXperiments and Technologies (CoNEXT)*, page 14, 2015.

[32] Masoud Moshref, Minlan Yu, Ramesh Govindan, and Amin Vahdat. Trumpet: Timely and precise triggers in data centers. In *Proceedings of the conference of the ACM Special Interest Group on Data Communication (SIGCOMM)*, pages 129–143, 2016.

[33] Srinivas Narayana, Anirudh Sivaraman, Vikram Nathan, Prateesh Goyal, Venkat Arun, Mohammad Alizadeh, Vimalkumar Jeyakumar, and Changhoon Kim. Language-directed hardware design for network performance monitoring. In *Proceedings of the conference of the ACM Special Interest Group on Data Communication (SIGCOMM)*, pages 85–98, 2017.

[34] Boyang Peng, Mohammad Hosseini, Zhihao Hong, Reza Farivar, and Roy Campbell. R-storm: Resource-aware scheduling in storm. In *Proceedings of the Annual Middleware Conference*, pages 149–161, 2015.

[35] Hooman Peiro Sajjad, Ken Danniswara, Ahmad Al-Shishtawy, and Vladimir Vlassov. Spanedge: Towards unifying stream processing over central and near-the-edge data centers. In *Proceedings of the IEEE/ACM Symposium on Edge Computing (SEC)*, pages 168–178, 2016.

[36] Anshu Shukla and Yogesh Simmhan. Model-driven scheduling for distributed stream processing systems. *Journal of Parallel and Distributed Computing*, 117:98–114, 2018.

[37] Praveen Tammana, Rachit Agarwal, and Myungjin Lee. Distributed network monitoring and debugging with SwitchPointer. In *Proceedings of the USENIX Symposium on Networked Systems Design and Implementation (NSDI)*, pages 453–456, 2018.

[38] Tong Yang, Jie Jiang, Peng Liu, Qun Huang, Junzhi Gong, Yang Zhou, Rui Miao, Xiaoming Li, and Steve Uhlig. Elastic sketch: Adaptive and fast network-wide measurements. In *Proceedings of the conference of the ACM Special Interest Group on Data Communication (SIGCOMM)*, pages 561–575. ACM, 2018.

[39] Minlan Yu, Lavanya Jose, and Rui Miao. Software defined traffic measurement with OpenSketch. In *Proceedings of the USENIX Symposium on Networked Systems Design and Implementation (NSDI)*, pages 29–42, 2013.

[40] Lihua Yuan, Chen-Nee Chuah, and Prasant Mohapatra. ProgME: towards programmable network measurement. *IEEE/ACM Transactions on Networking*, 19(1):115–128, 2011.

[41] Haoyu Zhang, Ganesh Ananthanarayanan, Peter Bodik, Matthai Philipose, Paramvir Bahl, and Michael J Freedman. Live video analytics at scale with approximation and delay-tolerance. In *Proceedings of the USENIX Symposium on Networked Systems Design and Implementation (NSDI)*, pages 377–392, 2017.

[42] Haiquan Chuck Zhao, Ashwin Lall, Mitsunori Ogihara, Oliver Spatscheck, Jia Wang, and Jun Xu. A data streaming algorithm for estimating entropies of OD flows. In *Proceedings of the ACM SIGCOMM conference on Internet measurement (IMC)*, pages 279–290, 2007.

[43] Yu Zhou, Dai Zhang, Kai Gao, Chen Sun, Jiamin Cao, Yangyang Wang, Mingwei Xu, and Jianping Wu. Newton: Intent-driven network traffic monitoring. In *Proceedings of the ACM Conference on emerging Networking EXperiments and Technologies (CoNEXT)*, pages 295–308, 2020.

A Appendix: Application of Cluster Sampling

In this section, we discuss details of key equations enabling our scheduling approach's accuracy and latency tradeoffs. To maintain a self-contained discussion, some content is repeated from § 4.

A.1 Trading Off Accuracy

Given fixed scheduling epochs, we can trade off accuracy for reduced resource requirements by sampling a subset of the subepochs in which to execute a particular query. We leverage cluster sampling theory [29] to expose this tradeoff while maintaining accuracy goals. To simplify our discussion, we first consider the case where a query is executed in a single epoch and then expand to the case where a query is executed across multiple epochs.

Single Epoch Case. Consider the case where a particular query executes in n of the N total subepochs. Our goal is to estimate the value that would have resulted from running the query in all subepochs based only on these n subepoch results. First, we note that each subepoch defines a cluster of packets that traverse the switch during that subepoch. Next, since each query executes over every packet of the subepochs in which it is scheduled, we note that the subepoch results represent a sample of n of the N total subepoch clusters. To ensure that each subepoch has an equal probability of being sampled by a particular query, we shuffle subepochs prior to execution. Cluster sampling theory [29] then lets us estimate the results of these queries over the entire N subepochs as well as the error of this estimator based on the variance between the observed subepochs. For example, we can estimate a query that maintains a sum by

$$\hat{t} = \frac{N}{n}\sum_{i\in S} t_i$$

which has standard error

$$SE(\hat{t}) = N\sqrt{\left(1-\frac{n}{N}\right)\frac{s_t^2}{n}}$$

where S is the index set of which subepochs have been sampled, t_i is the query's result in the i-th subepoch, and s_t^2 is the sample variance of the t_i's. Clearly, executing a query for fewer subepochs leads to greater sampling error while executing a query in each subepoch leads to zero sampling error. This equation also shows that, if n is set to a fixed ratio of N, error grows as a function of N so we do not expect to increase accuracy by dividing epochs into larger numbers of subepochs. Corresponding theory and equations exist for other update operations such as averages and extreme values.

Multiple Epoch Case. Due to changing traffic distributions or large query workloads, a query may not be able to fulfil its accuracy goal in a single epoch and the scheduler must form results based on the estimates from multiple epochs. Considering again the sum example, let $t_{i,j}$ be the query's result in the i-th subepoch of the j-th epoch, n_j be the number of subepochs in which the query executed in the j-th epoch, and E be the total number of epochs in which the query is executed. By the self-weighting property of $\hat{t}$, we can take a simple mean of the $\hat{t}_j$'s to get an unbiased estimator of the query's result over the E epochs,

$$\hat{t}_E = \frac{1}{E}\sum_{j=1}^{E}\hat{t}_j = \frac{1}{E}\sum_{j=1}^{E}\frac{N}{n_j}\sum_{i\in S_j} t_{i,j} \tag{5}$$

which has standard error

$$SE(\hat{t}_E) = \frac{N}{E}\sqrt{\sum_{j=1}^{E}\left(1-\frac{n_j}{N}\right)\frac{s_{t_j}^2}{n_j}} \tag{6}$$

because subepochs are chosen independently in each epoch (*i.e.*, the sampled index sets S_j, which are the only random variables in this formulation, are independent).

Application to Scheduling. Our system uses the point estimates provided by Equation 5 to calculate estimated query results. We also utilize Equation 6 for two purposes: (i) determining when accuracy goals have been fulfilled and (ii) estimating the number of subepochs in which the scheduler must execute particular queries. Since the first item can be evaluated with a simple threshold check, the rest of this section explains the second item. We assume that each query executes a single update operation (*e.g.*, a sum) in its reduction and note that multiple operations could be expressed in multiple queries.

Note that for a given standard error target ($SE(\hat{t}_E) = \sigma$) we can rearrange Equation 6 to solve for the number of subepochs that must be sampled in the E-th epoch as follows,

$$n^{acc} = \frac{s_{t_E}^2 N^2}{E^2\sigma^2 - \left(\sum_{j=1}^{E-1}\mathrm{Var}\left(\hat{t}_j\right)\right) + N s_{t_E}^2} \tag{7}$$

Given a query's target standard error σ, observed values of $s_{t_j}^2$ and n_j from prior epochs, and an estimate of $s_{t_E}^2$ (based on the $s_{t_j}^2$'s), we can use Equation 7 to determine a lower bound on the number of subepoch in which a query should execute. Note that if $\sigma = 0$, then $n^{acc} = N$ and the query will be executed in all of the subepochs in its first epoch. As σ

increases, n^{acc} decreases freeing more of the subepochs for other queries. For example, Figure A.1a shows the result of evaluating Eq. 7 for the first epoch of a query, indicating that if the accepted standard error is large enough, the scheduler only needs to execute the query in a single subepoch.

Limitations. We note that Equation 7 can become unstable when the accuracy goal σ cannot be obtained in a single epoch given the results of prior epochs. This condition results when $E^2\sigma^2 + Ns^2_{t_E} \leq \sum_{j=1}^{E-1} \text{Var}(\hat{t}_j)$ causing the value of n^{acc} to be negative or undefined. Moreover, when n^{acc} is negative, its magnitude has the wrong sense with respect to σ: smaller (tighter) values of σ reduce the magnitude of n^{acc}. Rather than dropping the query, we make a maximum allocation choice ($n^{acc} = N$) and retain the query for future epochs until its accuracy target is met. So long as $\text{Var}(\hat{t}_j) < \sigma^2$ for enough of those future epochs, n^{acc} will eventually stabilize.

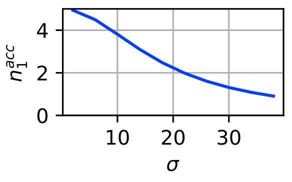

(a) Increasing σ reduces n^{acc} in the first epoch.

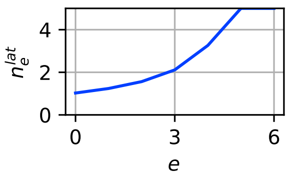

(b) n^{lat} increases as deadline $E = 6$ approaches.

Figure A.1: Numeric evaluations of Eqs. 7 and 8 assuming fixed variance $s_t^2 = 8$, $N = 5$, and queries get 3/5th of the subepochs.

A.2 Trading Off Latency

In addition to the accuracy tradeoff discussed above, we can tradeoff result latency for reduced resource requirements by executing a query's operations across several epochs. The key observation enabling this tradeoff is that by spreading the sampled subepochs over several epochs, the query can reduce its per-epoch requirements while still attaining its accuracy goal. Operators leverage this tradeoff by specifying larger latency goals on queries which do not require fast returns. We then adapt Equation 6 to estimate how many subepochs should be executed in the current epoch based on both past and anticipated future results.

Accounting for Past and Future Results. Under the latency tradeoff, we approach the problem of determining how many subepochs to execute from the perspective of the point in the future when the query completes. At this point Equation 5 will be used to estimate the query's result and Equation 6 must satisfy the query's accuracy goal. Moreover, assuming we are satisfying the query's latency goal, E is equal to the target number of epochs.

Now we consider the task of estimating the number of subepochs to execute during some epoch e before the query's final epoch E. Note that the sum in Equation 6 can be split around epoch e into a past component

$$past = \sum_{j=1}^{e-1} \left(1 - \frac{n_j}{N}\right) \frac{s^2_{t_j}}{n_j}$$

and a future component

$$future = \sum_{j=e+1}^{E} \left(1 - \frac{n_j}{N}\right) \frac{s^2_{t_j}}{n_j}.$$

We can then directly adapt Equation 7 to provide the required number of subepoch in epoch e accounting for both past and future components as

$$n^{lat} = \frac{s^2_{t_E} N^2}{E^2\sigma^2 - N^2(past + future) + Ns^2_{t_E}} \tag{8}$$

Figure A.1b shows the result of evaluating Equation 8 in each epoch leading up to a query's target latency of $e = 6$ assuming that the operation gets 3/5th of the number of subepochs requested in each epoch. Since in this case, the query is not given its full requested number of subepochs, the target n^{lat} increases dynamically to meet the deadline. This indicates that Equation 8 can dynamically drive scheduling decisions even when its results are not taken literally in each epoch (as may be the case when multiple queries compete for resources).

Limitations. Equation 8 faces the same issues as Equation 7 in that it may still be infeasible to satisfy σ given past results and the anticipated gains of future results. In such cases we again take $n_j = N$ and count on gaining sufficient resources in future epochs to satisfy the accuracy goal. To understand the dynamics of this decision, Figure A.2 shows the relation between target and actual number of epochs for a number of accuracy goals. We assume here that queries anticipate getting 3/5th of the subepochs, actually receive 3/5th of what they ask for, and all other settings are as in Figure A.1. As can be seen when the accuracy target is too tight (*e.g.*, $\sigma = 6$) executing in less than a certain number of epochs ($e = 5$) is infeasible and the query's latency goal cannot be met.

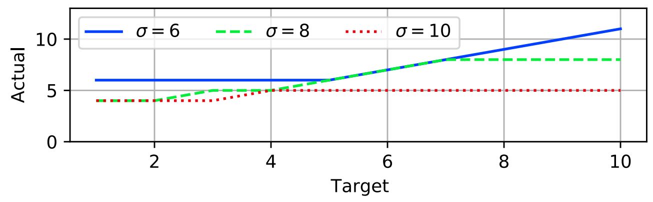

Figure A.2: Relation between target number of epochs and the actual required number of epochs.

A.3 Correcting Distinct Operators

Many useful queries also involve identifying and counting distinct elements. We consider the particularly prominent query structure where the results of a distinct operator are fed through a reduce operator with a slightly coarser granularity key. For example the DDoS query considered in § 2.1 contains two main stateful operators: (i) finding distinct source, destination pairs and (ii) reducing with destination as the key to count the number of unique sources contacting each destination. The key problem is that, while the methods above provide sound estimators for packet and byte counts, they do not correct for elements which may have been entirely missed in the distinct operator due to sampling. Such errors lead to a downward bias on distinct counts based on sampling which could cause key events like DDoS attacks to go unnoticed. To correct for this source of error, we leverage the Chao estimator without replacement when performing reductions after distinct operators impacted by sampling. Chao estimators [11, 12] are commonly used by "species richness" studies in the biological sciences to solve a related type of distinct count problem [21]

This estimator is given by

$$\hat{S}_{Chao1,wor} = S_{obs} + \frac{f_1^2}{\frac{n}{n-1} 2 f_2 + \frac{q}{1-q} f_1} \tag{9}$$

where S_{obs} is the number of elements observed in the sample, f_1 is the number of elements observed only once, f_2 is the number of elements observed only twice, n is the total number of elements in the sample, and q is the sampling rate. To use this estimator, we modify distinct operators executed in the data plane to additionally count the number of packets observed for each distinct element (essentially transforming them into normal count reduction operators). After gathering results, we can then easily compute the inputs required by Equation 9. Note that the variance of $\hat{S}_{Cha1,wor}$ can also be easily obtained from the same information as shown in the original description of this estimator [12], providing network operators with approximate accuracy of these results as well.